Structure, Vol. 12, 765–773, May, 2004, ©2004 Elsevier Science Ltd. All rights reserved. DOI 10.1016/j.str.2004.02.037

# Protein Regulation of Carotenoid Binding: Gatekeeper and Locking Amino Acid Residues in Reaction Centers of *Rhodobacter sphaeroides*

**Aleksander W. Roszak,[1] Kimberley McKendrick,[2] Alastair T. Gardiner,[2] Iain A. Mitchell,[1,2] Neil W. Isaacs,[1] Richard J. Cogdell,[2] Hideki Hashimoto,[3] and Harry A. Frank,[4,*]**
[1]Department of Chemistry
[2]Division of Biochemistry and Molecular Biology
IBLS
University of Glasgow
Glasgow G12 8QQ
United Kingdom
[3]Light and Control
PRESTO/JST
Department of Physics
Graduate School of Science
Osaka City University
3-3-138 Sugimoto
Sumiyoshi-ku
Osaka 558-8585
Japan
[4]Department of Chemistry
University of Connecticut
55 North Eagleville Road
Storrs, Connecticut 06269

## Summary

**X-ray diffraction was used to determine high-resolution structures of the reaction center (RC) complex from the carotenoidless mutant, *Rb. sphaeroides* R-26.1, without or reconstituted with carotenoids. The results are compared with the structure of the RC from a semiaerobically grown *Rb. sphaeroides* strain 2.4.1. The investigation reveals the structure of the carotenoid in the different protein preparations, the nature of its binding site, and a plausible mechanism by which the carotenoid is incorporated unidirectionally in its characteristic geometric configuration. The structural data suggest that the accessibility of the carotenoid to the binding site is controlled by a specific "gatekeeper" residue which allows the carotenoid to approach the binding site from only one direction. Carotenoid binding to the protein is secured by hydrogen bonding to a separate "locking" amino acid. The study reveals the specific molecular interactions that control how the carotenoid protects the photosynthetic apparatus against photo-induced oxidative destruction.**

## Introduction

Reaction center complexes isolated from purple nonsulfur photosynthetic bacteria contain a bacteriochlorophyll (BChl) dimer as a primary electron donor (P), two monomeric accessory BChls ($BChl_A$ and $BChl_B$), two bacteriopheophytins ($\phi_A$ and $\phi_B$), and two quinones ($Q_A$ and $Q_B$) (Blankenship et al., 1995; Clayton and Sistrom, 1978). Also, all RCs from naturally occurring species of photosynthetic bacteria contain a carotenoid molecule bound in a 1:1 stoichiometric ratio with P (Boucher et al., 1977; Cogdell et al., 1976). When light is absorbed, the excited singlet state P* becomes oxidized, and the electron acceptors become reduced in a succession of one-electron transfer reactions. Under redox conditions in which the quinones are reduced, or in RCs lacking quinones, the primary photochemistry is blocked, and the photoinduced charge separated state of $P^+\phi_A^-$ undergoes a rapid back reaction in which some of the RCs form a triplet state on P (Blankenship and Parson, 1979; Hoff, 1979; Kirmaier and Holten, 1987). The triplet state that forms on P is quenched in ~10 ns by the bound carotenoid, and this is an essential function of this molecule. If chlorophyll (Chl) or BChl triplet states are formed by illumination in an aerobic environment, the $^1\Delta_g$ singlet state of oxygen may be produced. This state of molecular oxygen is a powerful oxidizing agent capable of killing cells by inducing damage to proteins, lipids, and DNA (Krinsky, 1971). Carotenoids prevent oxidative destruction by rapidly quenching the sensitizing triplets before they can initiate this route of photo-impairment (Foote et al., 1970; Krinsky, 1971).

Reaction centers from the bacterium *Rhodobacter (Rb.) sphaeroides* provide a valuable opportunity to explore the molecular details controlling the involvement of carotenoids in the process of photoprotection. This is because the structure of this protein has been determined by X-ray diffraction (Allen et al., 1988; Arnoux et al., 1989; Chang et al., 1986, 1991; Ermler et al., 1994; Feher et al., 1989; Komiya et al., 1988; McAuley et al., 2000; Yeates et al., 1988), and RCs from the carotenoidless strain R-26.1 can be reconstituted with carotenoids having different conjugated chain lengths and functional group substitutions (Agalidis et al., 1980; Chadwick and Frank, 1986; Frank et al., 1986). For example, spheroidene may be readily incorporated into R-26.1 RCs, where it exhibits the same spectroscopic and functional characteristics of natural spheroidene in *Rb. sphaeroides* wild-type strain 2.4.1 (Agalidis et al., 1980; Chadwick and Frank, 1986; Frank et al., 1986; Frank and Violette, 1989). Spectroscopic studies on this and other carotenoid-containing *Rb. sphaeroides* RCs have established an essential role for $BChl_B$ in mediating triplet energy transfer (Chadwick and Frank, 1986; DeWinter and Boxer, 1999; Frank, 1990; Frank et al., 1986, 1993, 1996; Frank and Violette, 1989; Schenck et al., 1984; Takiff and Boxer, 1988a, 1988b; Taremi et al., 1989) and have elucidated the energetic requirements. An implicit assumption in all of these studies, however, is that the reconstituted carotenoid binds in the same position and with the same structure as the carotenoid in native RCs. High-resolution structures of these reconstituted RCs are needed to verify whether this is indeed the case.

This paper presents high-resolution structures of three RC protein complexes from the carotenoidless mutant, *Rb. sphaeroides* R-26.1, either without carotenoids or reconstituted with either spheroidene or 3,4-

*Correspondence: harry.frank@uconn.edu

Table 1. Data Collection and Refinement Statistics

| | R-26.1 Carotenoidless RC | R-26.1 Reconstituted with Spheroidene | R-26.1 Reconstituted with 3,4-Dihydro-Spheroidene |
|---|---|---|---|
| PDB ID code | 1RG5 | 1RGN | 1RQK |
| **Data Collection** | | | |
| Resolution range (Å) | 23.3–2.5 | 24.0–2.8 | 15.3–2.7 |
| Space group | $P3_12$ | $P3_12$ | $P3_12$ |
| Data measured at: | SRS Daresbury, Beamline 9.6 | ESRF Grenoble, Beamline ID14-3 | In-house rotating anode generator Nonius FR591 |
| Detector | ADSC Quantum4 | MAR CCD | MacScience DIP2020 |
| Temperature (K) | 298 | 100 | 298 |
| Cell (Å) (a = b, c) | 144.0, 190.1 | 139.8, 184.0 | 141.7, 187.2 |
| Unique reflections | 78,686 | 46,063 | 57,643 |
| Redundancy (last shell) | 4.7 (4.8) | 3.9 (3.5) | 2.1 (2.0) |
| Completeness (%) | 99.1 (99.0) | 89.0 (91.4) | 96.2 (95.1) |
| Average $I/\sigma$ | 11.0 (2.2) | 22.5 (3.2) | 7.3 (1.5) |
| $R_{merge}$[a] | 0.074 (0.864) | 0.055 (0.342) | 0.107 (0.786) |
| **Refinement** | | | |
| R factor[b] | 0.155 | 0.189 | 0.162 |
| $R_{free}$[b] | 0.182 | 0.232 | 0.194 |
| **Ramachandran Plot** | | | |
| Most favored and allowed regions/ disallowed regions (%) | 99.7/0.0 | 99.7/0.0 | 99.7/0.0 |
| Rms deviation bond lengths (Å) | 0.017 | 0.019 | 0.016 |
| Rms deviation bond angles (°) | 1.7 | 1.9 | 1.7 |
| Coordinate error[c] (Å) | 0.16/0.10 | 0.40/0.19 | 0.25/0.14 |
| No. of all atoms/water molecules refined | 7451/243 | 7289/173 | 7522/208 |
| Average/Wilson plot B factors (Å$^2$) | 52.9/57.4 | 70.6/79.5 | 47.6/53.0 |

Values in parentheses are for the highest resolution bin (approximate interval, 0.05 Å).
[a] $R_{merge} = \Sigma|I_{hkl} - <I_{hkl}>|/\Sigma I_{hkl}$.
[b] $R = \Sigma|F_o(hkl)| - |F_c(hkl)|/\Sigma|F_o(hkl)|$ for all data except for 5% that was used for the $R_{free}$ calculations.
[c] Estimated standard uncertainty; first value calculated using the method of Cruickshank (Cruickshank, 1999), second one based on maximum likelihood as implemented in REFMAC (Murshudov et al., 1997).

dihydrospheroidene (also known as methoxyneurosporene) (Table 1). The results are compared with the structure of the RC from a semiaerobically grown *Rb. sphaeroides* mutant strain AM260W (McAuley et al., 2000) containing spheroidenone (Figure 1). The *Rb. sphaeroides* AM260W mutant structure is our highest resolution structure of an RC that naturally contains a carotenoid and is ideal for this analysis. The AM260W mutation is in the $Q_A$ binding site on the opposite side of the RC from where the carotenoid is bound and introduces no changes to the RC protein in the vicinity of the carotenoid. The present study pays particular attention to the structure of the carotenoid and the nature of its binding site in the protein and reveals a novel mechanism by which the carotenoid binds to the protein unidirectionally in its characteristic 15-15′-*cis* geometric configuration. This information is important for elucidating the role the protein plays in controlling the high efficiency of triplet energy transfer from the primary donor to the carotenoid in RCs and for understanding how the protein uses carotenoids as protective devices against photooxidation.

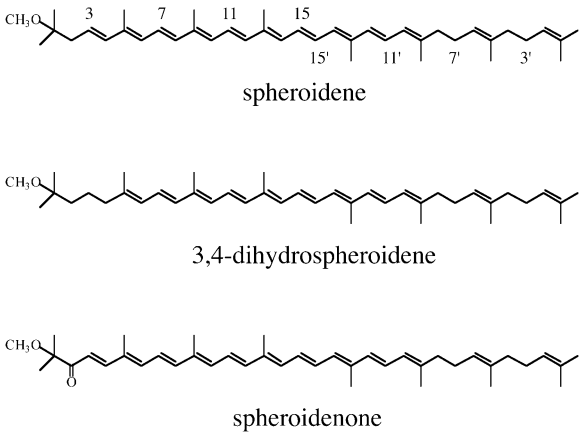


Figure 1. The Structures of the Carotenoids in the RCs Studied in the Present Work

## Results and Discussion

Reaction centers isolated from semiaerobically grown *Rb. sphaeroides* wild-type contain a spheroidenone molecule (Figure 1) residing ~11 Å from the primary electron donor and in van der Waals contact with the accessory $BChl_B$ (Figure 2) (McAuley et al., 2000). If the *Rb. sphaeroides* cells are grown anaerobically, the RCs contain spheroidene (Figure 1) in the same location (Arnoux et al., 1989; Yeates et al., 1988). In both of these

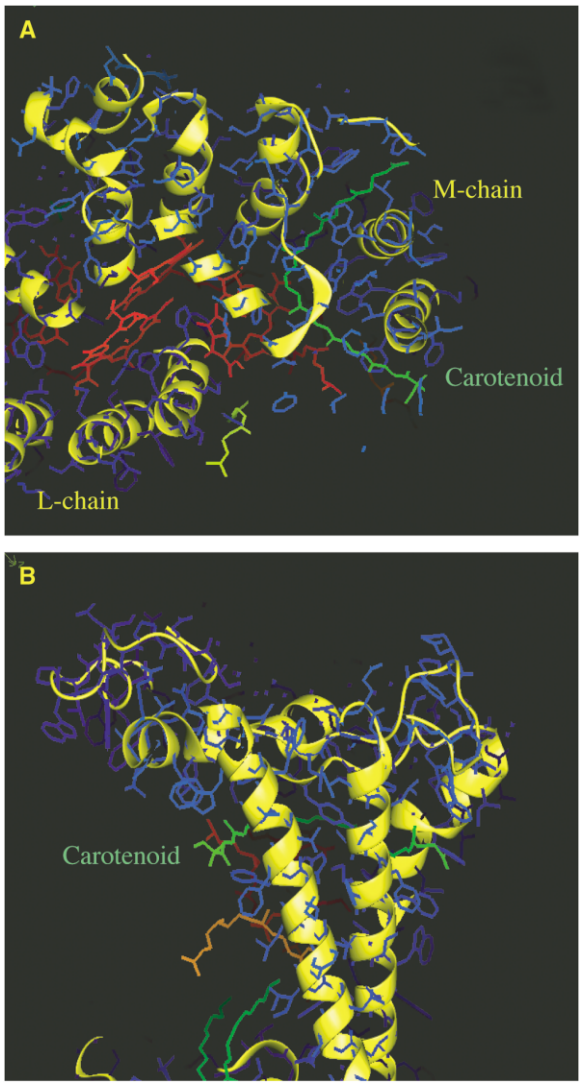


Figure 2. Two Views of the Binding of the Carotenoid Spheroidenone, in Green, in the RC from the *Rb. sphaeroides* AM260W Mutant Determined at 2.1 Å Resolution

(A) Top view showing the proximity of the carotenoid to the BChl dimer, P, and the accessory $BChl_B$ (both in red), and its position relative to the $\alpha$ helices in the M subunit of the RC.

(B) Side view showing the protrusion of the methoxy-head and tail regions of the carotenoid from the protein. This view also shows that the carotenoid is located at the top, or at the edge, of the transmembrane region of the RC. The chain shown in orange is the phytol tail of $\phi_B$. This structure has PDB ID code 1QOV.

cases, the carotenoid adopts a 15-15′-*cis* geometric isomeric configuration (Figure 2A) and lies in a plane roughly parallel to the surface of membrane (Figure 2B). The carotenoid is located wholly within the M subunit of the RC complex and wraps itself around two transmembrane helices spanning residues M54–M77 and M114–M139, respectively (Figure 2A). The carotenoid is found between the second of these helices and a third transmembrane helix containing amino acids M145–M168. The carotenoid binding pocket is constructed from 29 amino acids and the accessory bacteriochlorophyll, $BChl_B$, all of which come within 4.5 Å of the carotenoid. The residues are listed in Table 2 together with their distances of closest approach and the contact surface areas between the atoms of the residues and the atoms of the carotenoid, spheroidenone. The values were calculated as described in (Sobolev et al., 1999) from the X-ray structure of the AM260W mutant of *Rb. sphaeroides* (McAuley et al., 2000; PDB ID code 1QOV) determined at 2.1 Å resolution. Twenty-three of the amino acids and the $BChl_B$ generate hydrophobic-hydrophobic, stabilizing contacts with the carotenoid. Among these are 15 aromatic amino acids, including 8 phenylalanines, 5 tryptophans, 1 tyrosine, and 1 histidine, which together comprise more than 50% of the ligand-protein complementarity surface area; the total theoretical surface of carotenoid in a 15-15′-*cis* configuration is ~1200 Å$^2$. $BChl_B$ has the largest single contribution in the carotenoid binding pocket (Table 2). The $BChl_B$ macrocycle and its phytol tail are in contact with the carotenoid. Nineteen residues possess some degree of hydrophobic-hydrophilic, destabilizing interactions with the carotenoid. Figure 3A shows the entire carotenoid binding site with the electron density for the AM260W mutant (McAuley et al., 2000). Figures 4A–4D show the close-up details in the "methoxy-head," "*cis*-bond," "end-of-conjugation," and "tail" regions of the carotenoid, respectively.

Table 2. Amino Acid Residues and Cofactors Comprising the Carotenoid Binding Site with the Distances of Closest Approach and Contact Surface Areas between the Atoms of the Residues and the Atoms of the Carotenoid, Spheroidenone

| | Distance of Closest Approach (Å) | Contact Surface Area (Å$^2$) |
|---|---|---|
| $BChl_B$ | 3.4 | 101.2 |
| Trp M66 | 4.0 | 14.8 |
| Phe M67 | 3.6 | 59.6 |
| Phe M68 | 3.2 | 39.9 |
| Ile M70 | 3.6 | 33.7 |
| Gly M71 | 3.3 | 28.5 |
| Ile M72 | 4.4 | 12.1 |
| Phe M74 | 3.5 | 46.4 |
| Trp M75 | 3.1 (H bond) | 45.2 |
| Phe M85 | 3.9 | 30.0 |
| Leu M89 | 4.1 | 9.2 |
| Phe M105 | 4.4 | 26.9 |
| Trp M115 | 3.7 | 31.2 |
| Leu M116 | 4.3 | 15.3 |
| Ser M119 | 3.5 | 36.6 |
| Phe M120 | 4.1 | 38.4 |
| Met M122 | 3.7 | 17.5 |
| Phe M123 | 4.2 | 38.8 |
| Trp M157 | 3.3 | 63.9 |
| Met M158 | 4.1 | 4.7 |
| Leu M160 | 3.8 | 30.5 |
| Gly M161 | 3.7 | 31.2 |
| Phe M162 | 3.8 | 44.6 |
| Trp M171 | 3.5 | 35.9 |
| Val M175 | 3.5 | 37.9 |
| Pro M176 | 4.5 | 1.1 |
| Tyr M177 | 3.7 | 52.0 |
| Gly M178 | 3.8 | 18.2 |
| Ile M179 | 3.7 | 30.1 |
| His M182 | 3.6 | 41.5 |

The values were calculated from the X-ray structure of the AM260W mutant of *Rb. sphaeroides* (McAuley et al., 2000; PDB ID code 1QOV) determined at 2.1 Å resolution.

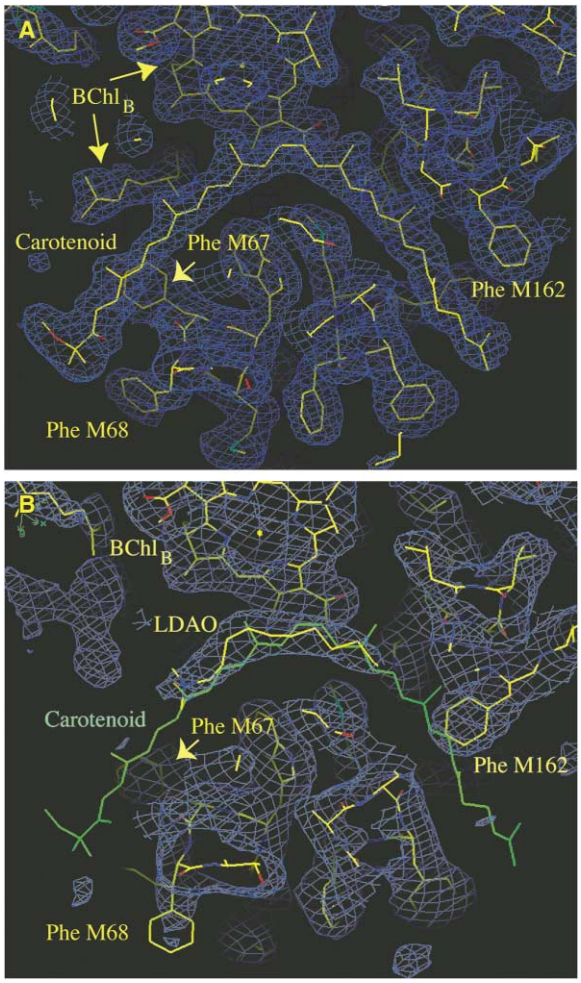


Figure 3. The Carotenoid Binding Site

The carotenoid binding site showing (A) the electron density for the AM260W mutant of *Rb. sphaeroides* containing spheroidenone (McAuley et al., 2000) and (B) the electron density and structure (in yellow) of the RC from the carotenoidless mutant *Rb. sphaeroides* R-26.1 in the absence of a bound carotenoid overlaid with the structure of spheroidenone (in green). Note that when the carotenoid is absent (in [B]), the binding site contains a single LDAO detergent molecule and the "gatekeeper" Phe M162 side chain. This conformation of Phe M162 contrasts with that shown in (A), where, in the presence of the carotenoid, it is found in an alternate position outside the binding site. Note also the locations of the $BChl_B$ phytol tail and Phe M67 (in [A]), which stabilize the carotenoid in place. This structure has PDB ID code 1QOV.

Both ends of carotenoid molecule in *Rb. sphaeroides* RCs are solvent accessible in the crystal structure (see Figure 2), but these areas constitute only about 15% of the carotenoid complementarity surface. The hydrophilic methoxy-head of spheroidenone is involved in a single carotenoid-protein hydrogen bonding interaction formed between the methoxy oxygen of carotenoid and the hydrogen on the indole group N atom of Trp M75. The $O_{Car}$–$N_{M75}$ distance was found to be 3.3 Å for spheroidenone, 2.9 Å for spheroidene, and 3.4 Å for 3,4-dihydrospheroidene. The orientation of the Trp M75 side chain is held in place by a $\pi$-$\pi$ stacking interaction with the Phe M85 (Figure 4A). This is the only position in which Trp M75 can reside; otherwise it would clash with the protein. Thus, neighboring residues are responsible for positioning Trp M75 in a suitable conformation for hydrogen bonding to the carotenoid. Also, this region of the carotenoid binding site involving Trp M75 and Phe M85 is very ordered. In contrast, on the opposite side of the carotenoid binding site, Phe M67 and Phe M68 (see Figure 4A) are able to adopt a number of conformations in the carotenoidless RC, which suggests that they can adjust their positions to allow the carotenoid easier access to the binding site.

The hydrogen bond involving Trp M75 is probably the most energetically stable single protein contact for carotenoid binding, and as suggested by previous structures (Arnoux et al., 1989; Chirino et al., 1994; McAuley et al., 2000), it is very important for "locking" the carotenoid in its site and ensuring secure, unidirectional binding. Carotenoids lacking the methoxy group are often removed during purification of the RCs (R.J.C., unpublished data). Analyses of the carotenoid composition of whole cells of *Rb. sphaeroides* strain GA reveal that three primary carotenoids, neurosporene, chloroxanthin, and 3,4-dihydrospheroidene, are present in the percent ratio 48:37:14 (Takaichi, 1999). Neurosporene lacks an oxygenated functional group, chloroxanthin has a hydroxy-head group, and 3,4-dihydrospheroidene has a methoxy-head group (Figure 1). Analysis of the pigment composition of RCs isolated from this strain shows that 3,4-dihydrospheroidene is bound in 94% of the RCs isolated from this strain (Cogdell, 1978), illustrating the importance of the methoxy-head group in binding. Also, apparently the carbonyl group on spheroidenone is unimportant to carotenoid binding, because it has no significant or obvious interactions with amino acid residues in the binding site.

Several regions of $\pi$-$\pi$ stacking interactions between the conjugated polyene portion of carotenoid and the aromatic amino acid side chains, and the $BChl_B$, stabilize the carotenoid binding in addition to hydrogen bonding to Trp M75. The most important of these is the interaction between the 15-15′-*cis* double bond region of the carotenoid and the acetyl group and the peripheral carbon-carbon $\pi$ bond of ring I of the $BChl_B$ macrocycle (Figures 2A and 4B). Although the conjugated planes of the $BChl_B$ and the carotenoid are not exactly parallel (dihedral angle $\sim$20°), the distances between their atoms in the overlapping region are in the 3.2–3.4 Å range. This relative arrangement of carotenoid and the $BChl_B$ macrocycle is critical for the effectiveness of the triplet quenching properties of carotenoid, because triplet-triplet energy transfer requires van der Waals contact between pigments for efficient electron exchange (Dexter, 1953). $\pi$-$\pi$ stacking interactions are also found near the end-portion of the carotenoid conjugated system where the C11′-to-C9′ segment (see Figure 1) of the polyene chain comes in proximity to the indole ring of Trp M157 (Figure 4C). Here the dihedral angle between interacting moieties is $\sim$15°. A parallel arrangement is not possible due to presence of the C9′-methyl group of the carotenoid. However, there is still close distance between atoms C11′ and the nitrogen on Trp M157, which is 3.1 Å for spheroidenone, 3.0 Å for spheroidene, and 3.1 Å for 3,4-dihydrospheroidene. Another region

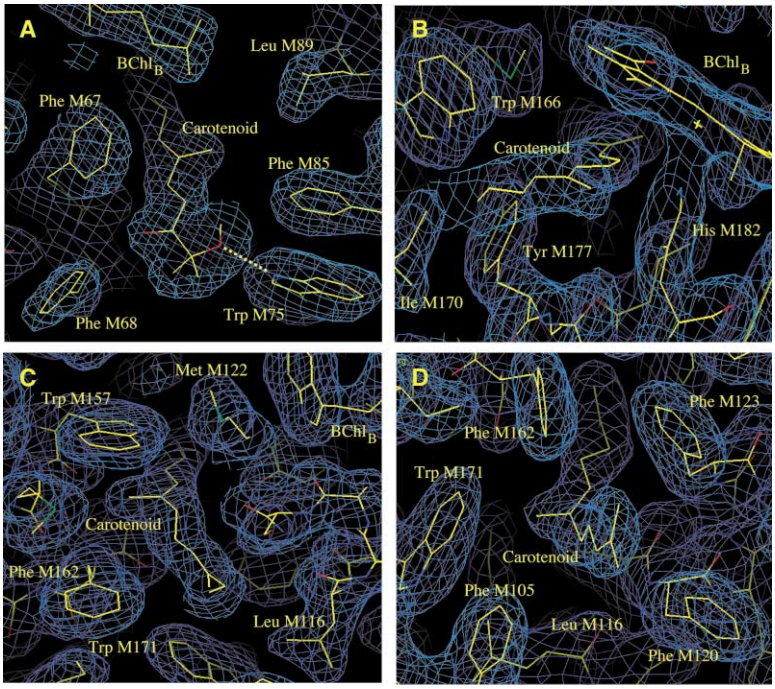


Figure 4. Close-up Details in Regions of the RC Binding Site Containing the Carotenoid, Spheroidenone

Close-up details in the (A) "methoxy-head", (B) "cis-bond", (C) "end-of-conjugation," and (D) "tail" regions of the RC binding site containing the carotenoid, spheroidenone. The dashed line in (A) corresponds to a hydrogen bond between the methoxy-head group of the carotenoid and Trp M75.

of potential $\pi$-$\pi$ stacking exists near the head portion of the carotenoid; viz. between the C4-C6 segment of the carotenoid and the phenyl ring of Phe M67 (Figures 3 and 4A). In this case, the dihedral angle between interacting conjugated planes is $\sim$40°, but the close distance of 3.3–3.5 Å between the nearest atoms in the overlapping regions suggests the presence of $\pi$-$\pi$ stacking interactions. This is most clear for the structure containing spheroidenone.

Comparisons of the structures of main chain atoms in the vicinity of the carotenoid binding site show that the structures are almost identical. Matching of the M55-M190 regions of the R-26.1 carotenoidless RC and the AM260W mutant RC reveals that the rms coordinate displacement for the main chain atoms is only 0.34 Å. Similar comparisons to the AM260W structure for R-26.1 RCs reconstituted with spheroidene or 3,4-dihydrospheroidene show average coordinate displacements of 0.29 and 0.16 Å, respectively. These values are not significant given the resolution and accuracies of the structures. Figure 5 shows the three carotenoid structures overlaid on top of each other as a result of these comparisons. It is important to note that the close agreement in the structures shown in the figure derives from overlaying the surrounding M chain protein and not from superimposing the carotenoid molecules themselves. Thus, it is clear that the 15-15′-*cis* bond is in an identical position relative to the BChl$_B$ macrocycle in both natural and carotenoid-reconstituted structures. The conformations of the three molecules differ slightly at the nonconjugated tail region and in the methoxy-head area. The methoxy group of the spheroidene molecule was found to be rotated by 180° relative to its orientation in the spheroidenone- and 3,4-dihydrospheroidene-containing structures but still forming a hydrogen bond to the M75-Trp indole group. This hydrogen bond, which has a $O_{Car}$–$N_{M75}$ distance of 2.9 Å, was found to be the shortest of all three RC proteins examined here. This set of disparate situations for the different carotenoid molecules indicates flexibility in the head region consistent with the variation in functional group substitutions, e.g., carbonyl, methoxy, hydroxy, etc., that are able to be accommodated by the protein.

When the carotenoid is absent from the RC, the carotenoid binding pocket is found to be smaller because the BChl$_B$ phytol tail adopts a different conformation directed away from the carotenoid site. This changes the shape of approximately one-third of the binding pocket from a tunnel to a solvent-accessible channel. The central portion of the pocket contains a stretch of electron density, which can be fitted with a single LDAO detergent molecule (Figure 3B). The carotenoid tail region of the pocket space has new electron density, which clearly indicates an alternative conformation to that found in carotenoid-containing RCs, of the phenylalanine side chain of residue M162. This conformation of the Phe M162 is the one most expected for phenylalanine side chains, it being found in $\sim$46% of phenylalanine residues in high-resolution protein structures (Ponder and Richards, 1987). However, this conformation would interfere sterically with the carotenoid if the carotenoid were also present in the binding site. Figure 3B illustrates this by showing the structure and electron density for the carotenoidless R-26.1 RC with the spheroidenone molecule overlaid where it is found in the AM260W mutant. When the carotenoid is bound, the phenylalanine side chain is rotated to a position outside the binding site (Figure 3A). Thus, Phe M162 acts as a "gatekeeper" residue, preserving the integrity and structure of the binding site in the absence of the carotenoid, yet having the ability to change its conformation and move away from the site when the carotenoid is pre-

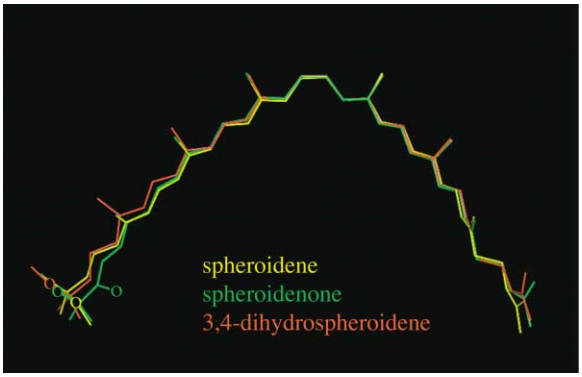


Figure 5. The Three Carotenoid Structures Discussed in the Text Overlaid by Matching the Surrounding M Chain Protein of the RC Proteins

The circles near the ends of the carotenoids correspond to oxygen atoms. Spheroidenone was present in RCs from the semiaerobically grown cells, whereas spheroidenone and 3,4-dihydrosperoidene were reconstituted into RCs isolated from R261.1.

sented for binding. A similar effect is not expected from the other two phenylalanines, Phe M123 and Phe M120, in the vicinity of the carotenoid tail because the most preferred conformations of these residues are not permitted owing to potential clashes with other M chain residues.

The crystal structures presented here show that reconstitution of spheroidene and 3,4-dihydrospheroidene into RCs prepared from the carotenoidless mutant *Rb. sphaeroides* R-26.1 lead to carotenoid binding very much the same as that found for natural spheroidenone. Most importantly, the position of the characteristic 15-15′-*cis* bond of the carotenoid relative to the $BChl_B$ macrocycle is virtually identical in all cases (see also Figure 5) and is in close proximity to it, as is required for triplet-triplet energy transfer from the primary donor to the carotenoid via the $BChl_B$ molecule.

The carotenoids used here for reconstitution into *Rb. sphaeroides* R-26.1 RCs are initially primarily in an all-*trans* geometric configuration because this is the dominant isomeric form for these carotenoids prepared either synthetically (3,4-dihydrospheroidene) or from extraction from *Rb. sphaeroides* wild-type cells (spheroidene). The dominance of the all-*trans* configuration in the cell extracts has been confirmed by high-performance liquid chromatography (Frank et al., 1997). Therefore, it is interesting to ask how the carotenoids structures are isomerized to the 15-15′-*cis*-isomeric form found in all RCs? One mechanism is that the RC protein acts as an isomerase. A carotenoid isomerase (CRTISO) enzyme exists in higher plants and cyanobacteria for the conversion of poly-*cis*-lycopene into the all-*trans* molecule (Isaacson et al., 2002). From the available *Rhodobacter* genomes, there does not appear to be any sequence closely related to the crtISO gene that codes for this enzyme. In any case, the enzyme is certainly not expected to be present in the purified RC solutions used in this work for reconstitution of the carotenoids. One could envision that the strength of binding of the carotenoid to the protein may be sufficient to overcome the barrier for *trans*-to-*cis* isomerization, but this barrier is rather high at ~70 kcal/mol (Morrison and Boyd, 1983). By analogy, in the retinal binding protein, rhodopsin, the protein is not able to generate the 11-*cis* isomer of retinal from the all-*trans* form even though the difference in binding energy for the 11-*cis* isomer is higher than the barrier to isomerization (Birge, 1981). Thus, it would be very unusual for the photosynthetic bacterial RC to induce isomerization of the carotenoid by simply binding the molecule to the protein. Also, although all-*trans* retinal does not bind to rhodopsin, the 11-*cis* and 9-*cis* isomers spontaneously enter the binding site (Birge, 1981). This may provide a clue to how the carotenoid binds to the RC. Regardless, the structural data presented here completely rule out the binding of the carotenoid to the RC in an all-*trans* form. There would be too many clashes with the protein. Moreover, the carotenoid binding site in the RC most certainly cannot accommodate the molecule undergoing a sweeping *trans*-to-15-15′-*cis* isomerization while bound to the protein.

An alternative interpretation for the mechanism by which carotenoids end up in a *cis*-isomeric form upon binding is that a fraction of the molecules are initially converted into the 15-15′-*cis* configuration before being incorporated. Thermal isomerization, which includes the processes of spontaneous isomerization at room temperature and isomerization upon heating in the absence of light or catalysts, can be very efficient, depending on the carotenoid and solvent system, and usually generates a distribution of several different geometric isomers (Koyama and Fujii, 1999; Kuki et al., 1991; Zechmeister, 1944). Thermal conversion of *trans* carotenoids into *cis* forms may be facilitated by sonication of the carotenoid/RC solution. This hypothesis was tested by preparing a solution of spheroidene in 15 mM Tris buffer (pH 8.0) containing 0.67% Triton X-100. One half of this solution was sonicated in the dark for 45 min while the other half was kept in the dark at room temperature and not sonicated. HPLC analysis of the two samples revealed 32% ± 9% more of the central-*cis*-isomer relative to the all-*trans* isomer in the sample that was sonicated compared to the one that was not. Sonication is obligatory to achieving a high level of incorporation of the carotenoid in the protein. The agitation may also facilitate reconstitution by opening the protein binding pocket for easier access by the carotenoid. The 15-15′-*cis* geometric isomer is one of the more stable configurations of carotenoids and could be selected from the distribution preferentially by the protein for binding. This would also be consistent with a several-fold molar excess of the carotenoid being required in the reconstitution procedure. It is also worthy of note that a locked-15-15′-*cis* isomer of spheroidene readily binds to R-26.1 RCs (Bautista et al., 1998), but attempts to reconstitute a locked-13-*cis*-spheroidene were unsuccessful (H.A.F. and J. A. Bautista, unpublished data).

The structure of the carotenoid binding site elucidated from the present studies provides a reasonable scenario for the path the carotenoid must take upon incorporation into the protein. The carotenoid must enter the protein from the Trp M75 side; otherwise, Phe M162, in its preferred conformation in the empty carotenoid binding site (Figure 3B), would not be able to move out of the way. Moreover, the bulky size of the methoxy-head group

suggests that the floppy tail of the carotenoid must be inserted first upon reconstitution. The carotenoid pushes past the gatekeeper residue, Phe M162, and is then fixed in place by a hydrogen bonding interaction between the methoxy group of the carotenoid and the indole hydrogen on the locking residue, Trp M75.

## Conclusions

The high-resolution structures of RC protein complexes with reconstituted carotenoids presented here reveal a remarkable similarity in the configurations of the bound carotenoids and the conformations of amino acid residues that comprise their protein binding sites. In addition, the structural data reveal a plausible mechanism for carotenoid insertion into the protein during reconstitution. Accessibility of the carotenoid to the binding site is controlled by Phe M162 acting as a gatekeeper, which allows the carotenoid to approach the binding site from only one direction. Secure carotenoid binding is ensured by hydrogen bonding to the locking residue, Trp M75, and a stabilizing interaction with the phytol tail of the $BChl_B$ molecule. Also, the mechanism by which the carotenoids bind to the protein in a characteristic 15-15′-*cis* configuration is indicated by these studies to be due to the preferential selection by the protein of the 15-15′-*cis* geometric configuration from the distribution of geometric isomers of the carotenoid present in solution.

## Experimental Procedures

### Cell Growth and Isolation of RCs

Reaction centers were prepared from *Rb. sphaeroides* R-26.1 cells grown anaerobically in modified Huntner's media (Cohen-Bazire et al., 1957) and purified according to the procedures described previously (Farhoosh et al., 1997).

### Incorporation of Carotenoids into the RCs from *Rb. sphaeroides* R-26.1

The spheroidene used in this study was extracted from anaerobically grown *Rb. sphaeroides* wild-type strain 2.4.1 and purified by column chromatography as previously published (Polívka et al., 2001). The 3,4-dihydrospheroidene was obtained by synthetic methods described in the literature (Gebhard et al., 1990, 1991; Marui et al., 2001). For reconstitution with spheroidene, RCs from *Rb. sphaeroides* R-26.1 were introduced into an 8 ml vial, and 1% of Triton X-100 in 15 mM Tris buffer (pH 8.0) was added to obtain a final solution of 0.67% Triton X-100. For reconstitution with 3,4-dihydrospheroidene, LDAO was used throughout in place of Triton X-100. A 15-fold molar excess of spheroidene or a 5-fold molar excess of 3,4-dihydrospheroidene in petroleum ether relative to BChl was layered onto the surface of the RC solution. The petroleum ether was then evaporated with a stream of nitrogen. The resulting mixture was sonicated for 30–45 min at room temperature in the dark. The solution was then diluted by a factor of five with 15 mM Tris buffer (pH 8.0) and loaded onto a 1 × 8 cm DEAE Sephacel column. The RCs containing the bound carotenoid were washed using a buffer containing 15 mM Tris, 0.1% Triton X-100, and 100 mM NaCl (at pH 8.0) to remove the excess unbound carotenoids. The purified RCs were then eluted using a buffer containing 15 mM Tris, 0.1% Triton X-100, and 300 mM NaCl (at pH 8.0) and dialyzed overnight using Spectrapor standard cellulose dialysis tubing (25 mm, M.W. cutoff 12,000–14,000 D) against 15 mM Tris buffer containing 0.03% Triton X-100 (at pH 8.0). Finally, the RCs with the carotenoid incorporated were concentrated for the crystallization trials by centrifugation at 3000 × g using an Amicon microconcentrator (MW cutoff of 10,000 D). The absorption spectra of *Rb. sphaeroides* R-26.1 RCs before and after reconstitution with the carotenoids have been published previously (Farhoosh et al., 1997; Frank, 1999).

### Crystallization of the Proteins

Crystals were grown by the sitting drop vapor diffusion method from droplets containing RCs at a final absorbance of 45 (at 800 nm in a 1 cm cell), 0.1% w/v LDAO, 3.5% w/v 1,2,3-heptanetriol, 0.35–0.50 M trisodium citrate, and 10 mM Tris HCl (pH 8.0) at a temperature of 16°C. The drops were equilibrated against a reservoir of 1.1–1.2 M trisodium citrate. 4% v/v ethylene glycol was added to some drops to ease the further addition of this substance used as a cryoprotectant in diffraction experiments carried out at 100 K. In these wells 0.4–0.5 M trisodium citrate was used as a precipitant, and 1.4–1.6 M trisodium citrate was placed in the reservoir. Crystals appeared within 1–4 weeks and grew as trigonal prisms of variable size ranging from 0.2 to 1.5 mm in the longest dimension, with the smaller ones appearing in the wells containing ethylene glycol.

### X-Ray Diffraction Data Collection, Processing, and Structure Refinement

The data processing and final structure refinement statistics are listed in Table 1. X-ray diffraction data for the carotenoidless R-26.1 RC and that reconstituted with 3,4-dihydrospheroidene were collected at room temperature using capillary mounted crystals. Samples were of trigonal prism morphology with the prism length of at least 1 mm to allow for multiple exposures in several separate portions of the crystal. Diffraction experiments for R-26.1 RCs reconstituted with spheroidene were performed at 100 K using smaller sized crystals. These were gradually equilibrated in mother liquors containing increasing concentrations of ethylene glycol (5%–30% v/v) before being looped and quickly placed in the stream of $N_2$ at 100 K. The effect of low temperature is evident in the smallest unit cell for this RC.

The data were indexed, integrated, and scaled using the HKL suite of programs (Otwinowski and Minor, 1997). All three structures were phased by molecular replacement using the program AMoRe (Navaza, 1994). The structure of the AM260W mutant of the RC from *Rb. sphaeroides* determined at 2.1 Å resolution (McAuley et al., 2000) was used as an initial model. Further processing was carried out using programs from the CCP4 package (CCP4, 1994). Manual rebuilding of the models was performed using QUANTA (Accelrys). In the cases of the carotenoidless RC and the RC reconstituted with 3,4-dihydrospheroidene, cardiolipin, LDAO detergent, heptane-1,2,3-triol, and water molecules were added manually into the $F_o$-$F_c$ electron density maps or with the use of the X-SOLVATE tool of QUANTA (Accelrys). In the case of the RC reconstituted with spheroidene, detergent and water molecules were identified and fitted, and a single phosphate ion was fitted in the cardiolipin binding region identified in the two other structures. All refinements have been carried out using a maximum likelihood method as implemented in REFMAC (Murshudov et al., 1997). As there is a strong correlation between occupancies and temperature factors, only the latter parameters were refined. The individual atomic temperature factors B were found to vary within the carotenoid structures. Their values for the atoms in central portions of carotenoids were close to the average B factor for all atoms of RC and for the atoms of the macrocycle of the relevant $BChl_B$. B factors for the atoms of the head and tail regions were higher.

These variations in B factors could be taken to represent the degree of flexibility in the carotenoid molecules and the effects of interactions between different parts of the carotenoids and their environments. The least flexibility and/or strongest interactions are therefore expected for the central portions of carotenoids where the *cis*-bond is the midpoint, while the head and tail portions show more flexibility or perhaps weaker interactions to the surrounding protein.

To account for the high anisotropy of the experimental diffraction data, the TLS (translation, libration, and screw tensors) thermal mode of refinement was employed (Winn et al., 2001). In this mode, first the TLS components are refined for selected groups of atoms or molecules to represent correlated atomic group motions. This is followed by the restrained refinement of atomic coordinates and isotropic B factors representing the residual thermal contributions, which cannot be modeled by TLS tensors. The whole asymmetric unit was assigned as a single TLS group in the structures reported here. This mode of refinement produced significant improvement

over the non-TLS isotropic refinement by lowering the crystallographic *R* factors and by improving electron density in disordered regions. The same TLS mode of refinement was also applied for further refinement of the structure of the AM260W mutant of *Rb. sphaeroides* RCs (McAuley et al., 2000) prior to its use as a starting model for molecular replacement calculations in this study (A.W.R., unpublished results). This produced a significant drop of R factors for the AM260W mutant structure from 16.9% to 13.6% for R and from 18.6% to 15.3% for $R_{free}$. More importantly, this produced improved electron density maps which allowed better tracing of the difficult regions at the RC surface, including the phytol tails of the $BChl_B$ and $\phi_B$ molecules. Unless otherwise stated, all further references to the structure of the AM260W mutant relate to the more fully refined structure (A.W.R., unpublished data). During all refinements, the models were monitored for geometrical quality using the program PROCHECK (Laskowski et al., 1993).

**Acknowledgments**

The authors wish to thank Drs. Paul Fyfe, Katherine McAuley, James Bautista, Ms. Pamela Dolan, and Ms. Amanda Deal for their help in the initial stages of this project, Mr. Takashi Marui for synthetic work, Mr. Zeus Pendon for carrying out the HPLC analysis of sonicated spheroidene samples, and Professors Robert Birge, Joseph Hirschberg, and Barry Pogson for useful discussions. This work was supported by grants from the National Institutes of Health (GM-30353 to H.A.F.), the National Science Foundation (MCB-0314380 to H.A.F.), NATO (to R.J.C. and H.A.F.), the BBSRC (R.J.C. and N.W.I.), Welcome Trust (N.W.I. and R.J.C.), NEDO (R.J.C. and H.H.), JSPS (H.H.), MEXT (H.H.) and JST (H.H.). H.A.F. also wishes to thank the University of Connecticut Research Foundation for sabbatical support during which time this manuscript was written.

Received: December 2, 2003
Revised: February 6, 2004
Accepted: February 8, 2004
Published: May 11, 2004

**References**

Agalidis, I., Lutz, M., and Reiss-Husson, F. (1980). Binding of carotenoids on reaction centers from *Rhodopseudomonas sphaeroides* R-26. Biochim. Biophys. Acta *589*, 264–274.

Allen, J.P., Feher, G., Yeates, T.O., Komiya, H., and Rees, D.C. (1988). Structure of the reaction center from *Rhodobacter sphaeroides* R-26 and 2.4.1. In The Photosynthetic Bacterial Reaction Center, J. Breton, and A. Vermeglio, eds. (New York: Plenum), pp. 5–11.

Arnoux, B., Ducruix, A., Reiss-Husson, F., Lutz, M., Norris, J., Schiffer, M., and Chang, C.-H. (1989). Structure of spheroidene in the photosynthetic reaction center from Y *Rhodobacter sphaeroides*. FEBS Lett. *258*, 47–50.

Bautista, J.A., Chynwat, V., Cua, A., Jansen, F.J., Lugtenburg, J., Gosztola, D., Wasielewski, M.R., and Frank, H.A. (1998). The spectroscopic and photochemical properties of locked-15,15′-cis-spheroidene in solution and incorporated into the reaction center of Rhodobacter sphaeroides R-26.1. Photosynth. Res. *55*, 49–65.

Birge, R.R. (1981). Photophysics of light transduction in rhodopsin and bacteriorhodopsin. Annu. Rev. Biophys. Bioeng. *10*, 315–354.

Blankenship, R.E., and Parson, W.W. (1979). The photochemical electron transfer reactions of photosynthetic bacteria and plants. In The Photochemical Electron Transfer Reactions of Photosynthetic Bacteria and Plants, J. Barber, ed. (New York: American Elsevier).

Blankenship, R.E., Madigan, M.T., and Bauer, C.E. (1995). Anoxygenic Photosynthetic Bacteria, Volume 2 (Dordrecht, Boston: Kluwer Academic Publishers).

Boucher, F., van der Rest, M., and Gingras, G. (1977). Structure and function of carotenoids in the photoreaction center from *Rhodospirillum rubrum*. Biochim. Biophys. Acta *461*, 3339–3357.

CCP4 (Collaborative Computational Project 4) (1994). The CCP4 suite: programs for protein crystallography. Acta Crystallogr. D *50*, 760–763.

Chadwick, B.W., and Frank, H.A. (1986). Electron-spin resonance studies of carotenoids incorporated into reaction centers of *Rhodobacter sphaeroides* R26.1. Biochim. Biophys. Acta *851*, 257–266.

Chang, C.H., Tiede, D., Tang, J., Smith, U., Norris, J., and Schiffer, M. (1986). Structure of *Rhodopseudomonas sphaeroides* R-26 reaction center. FEBS Lett. *205*, 82–86.

Chang, C.-H., El-Kabbani, O., Tiede, D., Norris, J., and Schiffer, M. (1991). Structure of the membrane-bound protein photosynthetic reaction center from *Rhodobacter sphaeroides*. Biochemistry *30*, 5352–5360.

Chirino, A.J., Lous, E.J., Huber, M., Allen, J.P., Schenck, C.C., Paddock, M.L., Feher, G., and Rees, D.C. (1994). Crystallographic analyses of site-directed mutants of the photosynthetic reaction center from *Rhodobacter sphaeroides*. Biochemistry *33*, 4584–4593.

Clayton, R.K., and Sistrom, W.R., eds. (1978). The Photosynthetic Bacteria (New York: Plenum Press).

Cogdell, R.J. (1978). Carotenoids in photosynthesis. Philos. Trans. R. Soc. Lond. Ser. B *284*, 569–579.

Cogdell, R.J., Parson, W.W., and Kerr, M.A. (1976). The type, amount, location, and energy transfer properties of the carotenoid in reaction centers from Rhodopseudomonas sphaeroides. Biochim. Biophys. Acta *430*, 83–93.

Cohen-Bazire, G., Sistrom, W.R., and Stanier, R.Y. (1957). Kinetic studies of pigment synthesis by non-sulfur purple bacteria. J. Cell. Comp. Physiol. *49*, 25–68.

Cruickshank, D.W.J. (1999). Remarks about protein structure precision. Acta Crystallogr. D Biol. Crystallogr. *55*, 583–601.

DeWinter, A., and Boxer, S.G. (1999). The mechanism of triplet energy transfer from the special pair to the carotenoid in bacterial photosynthetic reaction centers. J. Phys. Chem. B *103*, 8786–8789.

Dexter, D.L. (1953). A theory of sensitised luminescence in solids. J. Chem. Phys. *21*, 836–860.

Ermler, U., Fritzch, G., Buchanan, S.K., and Michel, H. (1994). Structure of the photosynthetic reaction centre from *Rhodobacter sphaeroides* at 2.65 Å resolution: cofactors and protein-cofactor interactions. Structure *2*, 925–936.

Farhoosh, R., Chynwat, V., Gebhard, R., Lugtenburg, J., and Frank, H.A. (1997). Triplet energy transfer between the primary donor and carotenoids in *Rhodobacter sphaeroides* R-26.1 reaction centers incorporated with spheroidene analogs having different extents of $\pi$-electron conjugation. Photochem. Photobiol. *66*, 97–104.

Feher, G., Allen, J.P., Okamura, M.Y., and Rees, D.C. (1989). Structure and function of bacterial photosynthetic reaction centers. Nature *339*, 111–116.

Foote, C.S., Chang, Y.C., and Denny, R.W. (1970). Chemistry of singlet oxygen. X. Carotenoid quenching parallels biological protection. J. Am. Chem. Soc. *92*, 5216–5218.

Frank, H.A. (1990). Potassium borohydride removes the monomeric bacteriochlorophyll and the carotenoid from reaction centers of *Rhodobacter sphaeroides* wild type strain 2.4.1. Trends Photochem. Photobiol. *1*, 1–4.

Frank, H.A. (1999). Incorporation of carotenoids into reaction center and light-harvesting pigment-protein complexes. In The Photochemistry of Carotenoids, H.A. Frank, A.J. Young, G. Britton, and R. J. Cogdell, eds. (Dordrecht: Kluwer Academic Publishing), pp. 235–244.

Frank, H.A., and Violette, C.A. (1989). Monomeric bacteriochlorophyll is required for the triplet energy transfer between the primary donor and the carotenoid in photosynthetic bacterial reaction centers. Biochim. Biophys. Acta *976*, 222–232.

Frank, H.A., Chadwick, B.W., Taremi, S., Kolaczkowski, S., and Bowman, M.K. (1986). Singlet and triplet absorption spectra of carotenoids bound in the reaction centers of *Rhodopseudomonas sphaeroides* R26. FEBS Lett. *203*, 157–163.

Frank, H.A., Chynwat, V., Hartwich, G., Meyer, M., Katheder, I., and Scheer, H. (1993). Carotenoid triplet state formation in *Rhodobacter sphaeroides* R-26 reaction centers exchanged with modified bacteriochlorophyll pigments and reconstituted with spheroidene. Photosynth. Res. *37*, 193–203.

Frank, H.A., Chynwat, V., Posteraro, A., Hartwich, G., Simonin, I., and Scheer, H. (1996). Triplet state energy transfer between the primary donor and the carotenoid in *Rhodobacter sphaeroides* R-26.1 reaction centers exchanged with modified bacteriochlorophyll pigments and reconstituted with spheroidene. Photochem. Photobiol. *64*, 823–831.

Frank, H.A., Desamero, R.Z.B., Chynwat, V., Gebhard, R., van der Hoef, I., Jansen, F.J., Lugtenburg, J., Gosztola, D., and Wasielewski, M.R. (1997). Spectroscopic properties of spheroidene analogs having different extents of $\pi$-electron conjugation. J. Phys. Chem. *101A*, 149–157.

Gebhard, R., Van der Hoef, K., Lefeber, A.W.M., Erkelens, C., and Lugtenburg, J. (1990). Synthesis and spectroscopy of (14′-$^{13}$C)- and (15′-$^{13}$C)spheroidene. Recl. Trav. Chim. Pays Bas *109*, 378–387.

Gebhard, R., Van Dijk, J.T.M., Van Ouwerkerk, E., Boza, M.V.T.J., and Lugtenburg, J. (1991). Synthesis and spectroscopy of chemically modified spheroidenes. Recl. Trav. Chim. Pays Bas *110*, 459–469.

Hoff, A.J. (1979). Applications of ESR in photosynthesis. Phys. Rep. *54*, 75–200.

Isaacson, T., Ronen, G., Zamir, D., and Hirschberg, J. (2002). Cloning of tangerine from tomato reveals a carotenoid isomerase essential for the production of beta-carotene and xanthophylls in plants. Plant Cell *14*, 333–342.

Kirmaier, C., and Holten, D. (1987). Primary photochemistry of reaction centers from the photosynthetic purple bacteria. Photosynth. Res. *13*, 225–260.

Komiya, H., Yeates, T.O., Rees, D.C., Allen, J.P., and Feher, G. (1988). Structure of the reaction center from *Rhodopseudomonas sphaeroides* R-26 and 2.4.1: symmetry relations and sequence comparisons between different species. Proc. Natl. Acad. Sci. USA *85*, 9012–9016.

Koyama, Y., and Fujii, R. (1999). Cis-trans carotenoids in photosynthesis: configurations, excited-state properties and physiological functions. In The Photochemistry of Carotenoids, H.A. Frank, A.J. Young, G. Britton, and R. J. Cogdell, eds. (Dordrecht: Kluwer Academic Publishers), pp. 161–188.

Krinsky, N.I. (1971). Function. In Carotenoids, O. Isler, G. Guttman, and U. Solms, eds. (Basel: Birkhauser Verlag), pp. 669–716.

Kuki, M., Koyama, Y., and Nagae, H. (1991). Triplet-sensitized and thermal isomerization of all-trans, 7-cis, 9-cis, 13-cis and 15-cis isomers of $\beta$-carotene: configurational dependence of the quantum yield of isomerization via the T1 state. J. Phys. Chem. *95*, 7171–7180.

Laskowski, R.A., MacArthur, M.W., Moss, D.S., and Thornton, J.M. (1993). Procheck: a program to check the stereochemical quality of protein structures. J. Appl. Crystallogr. *26*, 283–291.

Marui, T., Yamada, T., Kobayashi, T., and Hashimoto, H. (2001). Total synthesis and spectroscopic characterization of spherodiene analogues. Carotenoid Science *4*, 76–77.

McAuley, K.E., Fyfe, P.K., Ridge, J.P., Cogdell, R.J., Isaacs, N.W., and Jones, M.R. (2000). Ubiquinone binding, ubiquinone exclusion, and detailed cofactor conformation in a mutant bacterial reaction center. Biochemistry *39*, 15032–15043.

Morrison, R.T., and Boyd, R.N. (1983). Organic Chemistry, 4th Edition (New York: Allyn and Bacon).

Murshudov, G.N., Vagin, A.A., and Dodson, E.J. (1997). Refinement of macromolecular structures by the maximum-likelihood method. Acta Crystallogr. D Biol. Crystallogr. *53*, 240–255.

Navaza, J. (1994). AMORE—an automated package for molecular replacement. Acta Crystallogr. *A50*, 157–163.

Otwinowski, Z., and Minor, W. (1997). Processing of X-ray diffraction data collected in oscillation mode. Methods Enzymol. *276*, 307–326.

Polívka, T., Zigmantas, D., Frank, H.A., Bautista, J.A., Herek, J.L., Koyama, Y., Fujii, R., and Sundström, V. (2001). Near-infrared time-resolved study of the S1 state dynamics of the carotenoid spheroidene. J. Phys. Chem. B *105*, 1072–1080.

Ponder, J.W., and Richards, F.M. (1987). Tertiary templates for proteins: use of packing criteria in the enumeration of allowed sequences for different structural classes. J. Mol. Biol. *193*, 775–791.

Schenck, C.C., Mathis, P., and Lutz, M. (1984). Triplet formation and triplet decay in reaction centers from the photosynthetic bacterium *Rhodopseudomonas sphaeroides*. Photochem. Photobiol. *39*, 407–417.

Sobolev, V., Sorokine, A., Prilusky, J., Abola, E.E., and Edelman, M. (1999). Automated analysis of interatomic contacts in proteins. Bioinformatics *15*, 327–332.

Takaichi, S. (1999). Carotenoids and carotenogenesis in anoxygenic photosynthetic bacteria. In The Photochemistry of Carotenoids, H.A. Frank, A.J. Young, G. Britton, and R. J. Cogdell, eds. (Dordrecht: Kluwer Academic Publishing), pp. 39–69.

Takiff, L., and Boxer, S.G. (1988a). Phosphorescence from the primary donor in *Rhodobacter sphaeroides* and *Rhodopseudomonas viridis* reaction centers. Biochim. Biophys. Acta *932*, 325–334.

Takiff, L., and Boxer, S.G. (1988b). Phosphorescence spectra of bacteriochlorophylls. J. Am. Chem. Soc. *110*, 4425–4426.

Taremi, S.S., Violette, C.A., and Frank, H.A. (1989). Transient optical spectroscopy of single crystals of the reaction center from *Rhodobacter sphaeroides* wild-type 2.4.1. Biochim. Biophys. Acta *973*, 86–92.

Winn, M.D., Isupov, M.N., and Murshudov, G.N. (2001). Use of TLS parameters to model anisotropic displacements in macromolecular refinement. Acta Crystallogr. D Biol. Crystallogr. *57*, 122–133.

Yeates, T.O., Komiya, H., Chirino, A., Rees, D.C., Allen, J.P., and Feher, G. (1988). Structure of the reaction center from *Rhodopseudomonas sphaeroides* R-26 and 2.4.1: protein-cofactor (bacteriochlorophyll, bacteriopheophytin, and carotenoid) interactions. Proc. Natl. Acad. Sci. USA *85*, 7993–7997.

Zechmeister, L. (1944). Cis-trans isomerization and stereochemistry of carotenoids and diphenylpolyenes. Chem. Rev. *34*, 267–344.

## Accession Numbers

The atomic coordinates and structure factors have been deposited in the Protein Data Bank (PDB ID codes 1RG5, 1RGN, and 1RQK).